A Mammalian Cochlea-based RF Channelizing Filter

C. Galbraith*, R. White†, K. Grosh†, and G. M. Rebeiz*
*Radiation Laboratory, Electrical Engineering and Computer Science Department
†Mechanical Engineering Department, The University of Michigan, Ann Arbor, MI 48109 USA

***Abstract*— A new type of an RF channelizer-filter[1] has been developed at 20–90 MHz. The filter topology is derived from an electrical-mechanical analogy of the mammalian cochlea. The channelizer response retains the desirable features of the cochlea including multiple-octave frequency coverage, a large number of output channels with constant fractional bandwidth, and a high-order upper stop-band response. Results of a 20-channel, 20–90 MHz channelizer prototype are presented and agree well with theory.**

***Index Terms*— Channelizer, multiplexer, filter, cochlea, basilar membrane.**

I. Introduction

RF and microwave multiplexers with a large number of output ports—so-called *channelizers*—have always posed a challenging design problem. Waveguide-based solutions require extensive manual tuning and are bulky and expensive [1]. C. Rauscher developed a logarithmic-periodic microstrip multiplexer covering 5 contiguous channels at C- and X-band [2].

This work presents a different approach to planar channelizer design based on the mammalian cochlea allowing us to easily cover 3 octaves of frequency range and, in principle, 3 decades of frequency range. Application areas include A/D converters, wideband EW systems, radio astronomy, and spectroscopy.

II. Theory

The motivation for this work is the mammalian cochlea, the electro-mechanical transducer located in the inner ear (Fig. 1) which converts the acoustical energy (sound waves) into the nerve impulses sent to the brain. The cochlea is an amazing channelizing filter with approximately 3000 distinct channels over a three decade frequency range, and can distinguish frequencies which differ by less than 0.5%. The filtering characteristics of the cochlea rely on the propagation of a coupled fluid-structure wave that results in a localized spatial response for each frequency. The structure can be thought of as a series of parallel beams upon which a fluid rests (Fig. 2). The beams act as a continuum of resonators and have decreasing resonant frequencies along the length of the cochlear duct. An incoming acoustic wave is injected into the fluid at one end of the duct and travels down the length of the cochlea, interacting with the flexible membrane. At a specific location along the duct, dependent on the frequency of the sound, the mechanical impedance of the acoustic wave is matched and large levels of membrane motion result. This mechanical resonance results in considerable beam motion. The beams are connected to ionic gate channels and trigger nerve impulses to the brain to produce a sensation of hearing at a frequency corresponding to the location along the basilar membrane. Von Bekesy was the first to realize this, actually constructing analog models of the cochlea to explore this hypothesis [3]. Previous efforts on achieving cochlear-like filtering focused on using VLSI techniques to implement a circuit realization of a cochlear-mechanics model at audio frequencies [4], [5]. To our knowledge, the work presented here is the first attempt to create an RF channelizing filter using a model derived from cochlear mechanics.

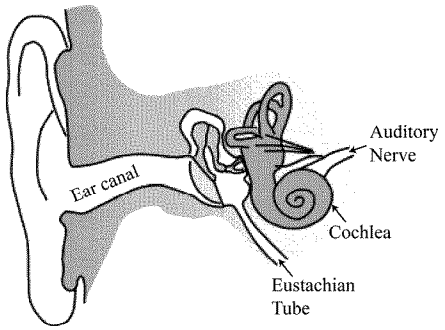

Fig. 1. The human auditory system. The basilar membrane is contained within the cochlea. (*Source:* http://en.wikipedia.org)

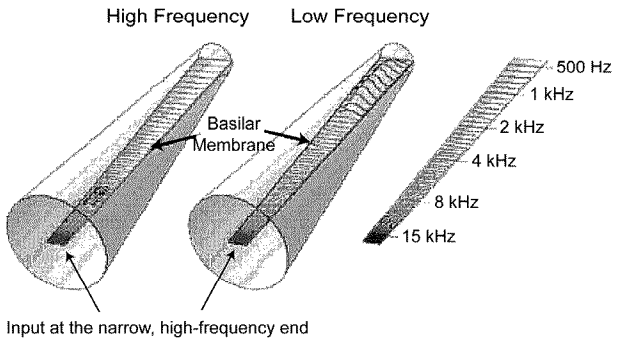

Fig. 2. The basilar membrane with input signal at high frequency (left) and low frequency (center).

In the simplest mechanical model of the cochlea, a one-dimensional fluid interacts with a variable impedance

[1]Patent application in process.

membrane, and the equation of motion is given by

$$\frac{d^2 v_{bm}}{dx^2} + \frac{\rho/Hk}{1 + j\omega\frac{r}{k} - \omega^2\frac{m}{k}}\omega^2 v_{bm} = 0 \qquad (1)$$

where v_{bm} is the basilar membrane transverse velocity, ρ is the fluid density, H is the height of the fluid duct, and k, m, and r are the membrane stiffness, mass, and damping, respectively. Note that v_{bm}, k, m, and r vary with position along the basilar membrane. This is a highly dispersive waveguide problem, where the coupled effects of the mechanical membrane and the fluid loading create the dispersion relation. The analogous equation for the electrical domain is a discretized, dispersive transmission line described by

$$\frac{d^2 V}{dx^2} + \frac{L_1 C}{1 - j\omega RC - \omega^2 L_2 C}\omega^2 V = 0 \qquad (2)$$

where V is the voltage along the transmission line, and L_1, L_2, C, and R correspond to the elements in Fig. 3. Note that V, L_1, L_2, C, and R are functions of position along the transmission line. In the analogy to the mechanical model, the series inductance L_1 plays the role of the fluid coupling and the shunt resonator elements L_2, C, and R play the role of the variable impedance (beam) structure.

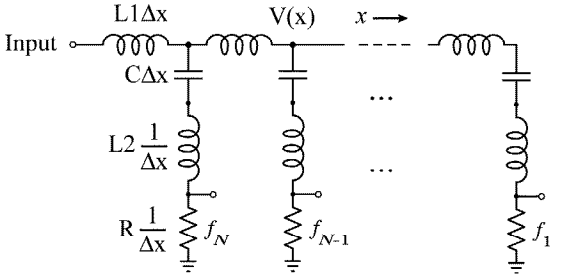

Fig. 3. Discretized transmission line model of the mammalian cochlea.

The channelizer operates as a low-pass t-line structure shunt-loaded by series-resonator sections. Each shunt resonator appears as a short-circuit at resonance and an open-circuit off resonance. The highest frequency channel resonator is located *closest* to the input, and the lowest channel frequency is located at the end of the t-line. Since the highest frequency components are removed from the input signal first, the rejection on the upper-side of the resonant frequency is much steeper than on the lower side. This response is characteristic of mammalian cochleas and is demonstrated later in simulated and measured results.

III. Design

The functional dependence between the coefficients in (1) and (2) is given by [7] and [6] and reduces the network design problem to the determination of four constants, α, A_1, A_2, and A_3, that relate L_1, L_2, C, and R by

$$L_2(x)C(x) = A_1 e^{\alpha x} \qquad (3)$$

$$R(x)C(x) = A_2 e^{0.5\alpha x} \qquad (4)$$

$$L_1(x)C(x) = A_3 e^{\alpha x} \qquad (5)$$

where x is the normalized transmission line length with $x = 0$ corresponding to the channelizer input. These constants are found by specifying four parameters: minimum channel frequency f_1, maximum channel frequency f_N, number of channels N, and the phase at each channel's center frequency θ referred to the channelizer input.

The channelizer design process begins by choosing four parameters: f_1, f_N, N, and θ. From these choices, all of the filter circuit elements are determined. The choice of θ is arbitrary and was originally chosen as 4π based on cochlear experimental data with acoustic waves. The choice of θ controls the input impedance of the channelizer since a larger θ requires a larger $L_1\Delta x$. In practice, one chooses the first three parameters then varies θ during simulation to arrive at an optimal input match.

The simulation is first done with ideal component values computed from the 1-D cochlea model described in (3)–(5). Then, the printed-circuit board (PCB) parasitics and true component values are used in the simulation of the actual channelizer.

IV. Experiment

A. 20-Channel, 20–90 MHz Channelizer

A 20-channel channelizer covering 20–90 MHz was designed, built, and measured (Figs. 4–6). The series induc-

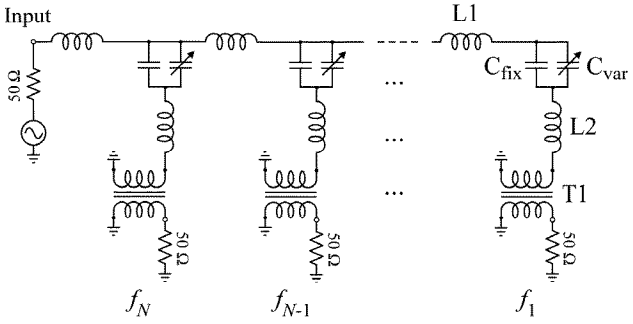

Fig. 4. Schematic diagram of the channelizer prototype. In this implementation, the resonator capacitances are formed by the parallel combination of C_{fix} and C_{var} to allow fine tuning.

tances L_1 are air-wound inductors with Q of 60–100 over the channelizer bandwidth. The shunt resonator sections are designed for a loaded Q of 16 and $|X_L|$=$|X_C|$=200 Ω at resonance, resulting in an effective impedance of 12.5 Ω. This is transformed to 50 Ω through a 1:2 turns ratio RF transformer at each channel output. The shunt resonator inductors L_2 are ceramic body wire-wound SMT components with Q of 25–40 at the channel center frequencies. To take into account the tolerance in the component values and since the capacitors and inductors are commercially

available in discrete values, the resonator capacitances C are implemented with the parallel combination of a fixed SMT capacitor and a coaxial trimmer capacitor. The total capacitor Q is greater than 200 over the channelizer bandwidth. Channelizer component design values range from 30 nH to 37 nH for L_1, 310 nH to 1570 nH for L_2, and 8 pF to 40 pF for C (Fig. 5). The circuit is

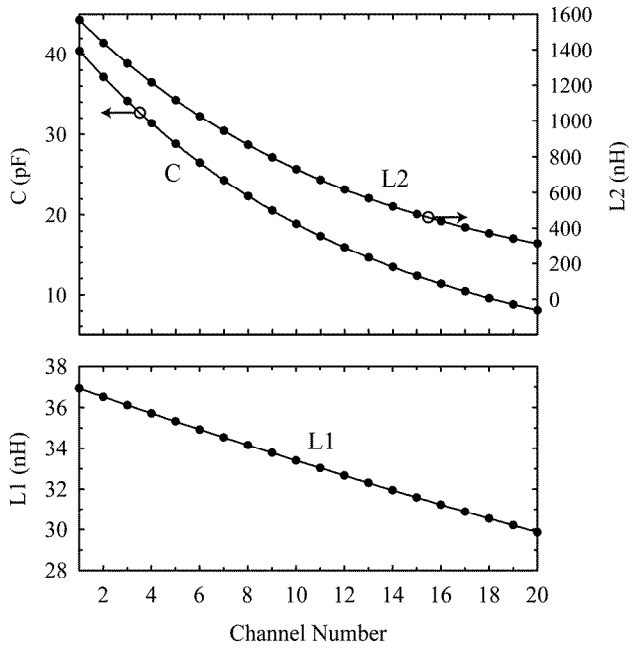

Fig. 5. Design values for L_1, L_2, and C for the 20–90 MHz filter.

constructed on a 61 mil FR4 PCB (Fig. 6) with the ground located along the perimeter of the PCB to reduce shunt parasitic capacitance. Simulations on two-sided PCB identified significant layout parasitics that gave undesirable spurious responses within the filter pass-band.

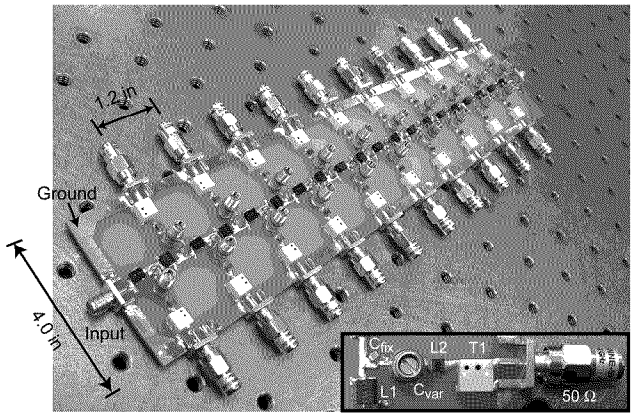

Fig. 6. Photograph of the 20-channel, 20–90 MHz channelizing filter. The inset shows a single channel layout with L_1, L_2, C, T_1 and 50 Ω termination.

B. Measurements

The channelizer is tuned by adjusting the trimmer capacitors on individual channel resonators until nulls in the measured S_{11} match the simulated response (Fig. 7). Channelizer measured and simulated S_{n1} (n=1–20) are

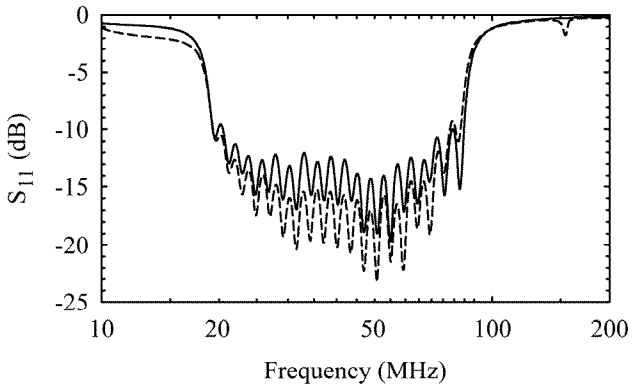

Fig. 7. Measured (solid) and simulated (dashed) S_{11} of the channelizing filter.

shown in Fig. 8. Also, a sample of three separate channel responses is shown in Fig. 9. Focusing on channel 10, we notice the characteristic cochlear response. The pass-band slope is first-order (20 dB/decade) below the channel center frequency and over fifth-order (100 dB/decade) immediately above the channel center frequency due to the low-pass nature of the dispersive transmission-line. The measured center frequencies and channel responses match simulation closely. Adjacent channel S_{21} cross at $\sim$ 2 dB below each channel's center frequency f_c (Table I). Each channel's 2 dB crossover bandwidth is 8.2±0.1%. Spurious responses above 100 MHz are due to resonances of the lumped inductors as well as PCB parasitic shunt capacitance.

TABLE I
CHANNELIZER CENTER FREQUENCIES (IN MHZ)

Ch	f_c	Ch	f_c	Ch	f_c	Ch	f_c
1	19.2	6	28.7	11	42.4	16	62.4
2	20.8	7	31.1	12	46.0	17	67.3
3	22.5	8	33.5	13	49.6	18	72.6
4	24.4	9	36.3	14	53.8	19	78.2
5	26.5	10	39.4	15	58.0	20	84.3

To understand the channelizer loss, consider the power distribution at the center frequency of channel 10 (39.4 MHz) (Table II). The percent of the input power appearing at the individual outputs is calculated from each channel's measured $|S_{21}|^2$. Likewise, the reflected power at the channelizer input is given by $|S_{11}|^2$. At 39.4 MHz, 33.2% of the power arrives at the channel 10 output (−4.8 dB),

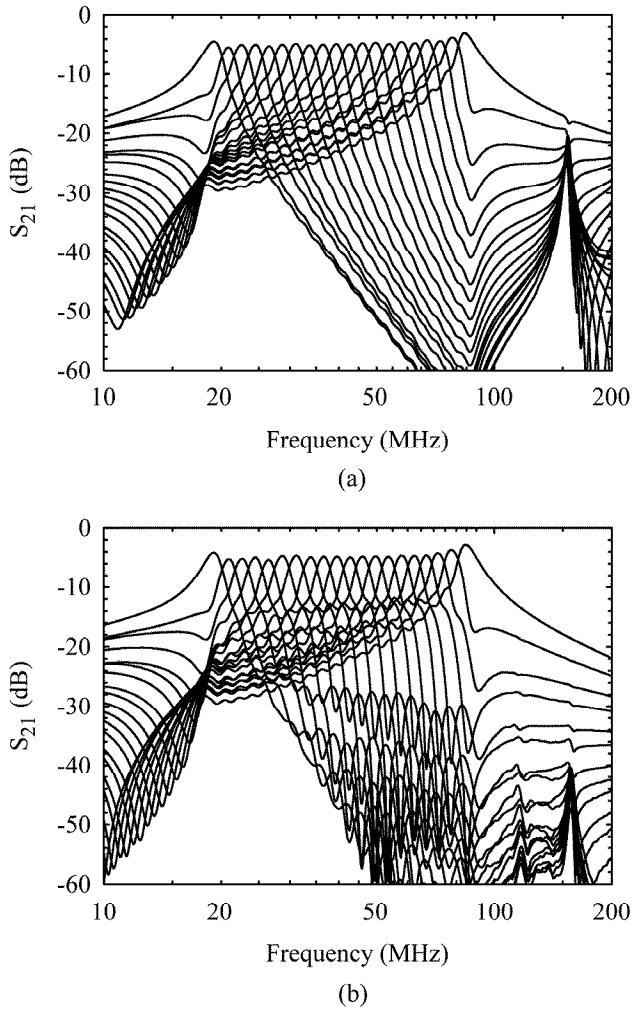

Fig. 8. (a) Simulated and (b) measured S_{n1} (n=1–20) of the channelizing filter.

32.3% appears at all other channel outputs (Fig. 10), and 3.5% is reflected at the channelizer input. Summing the powers results in 69.0% of the input power. Thus, the filter dissipates 31.0% of the input power corresponding to an effective loss of 1.6 dB.

Future work will concentrate on building a 200–1000 MHz and a 2–10 GHz channelizer using distributed techniques, and on taking this idea to 2-pole shunt resonators for a steeper cutoff and less power sharing between different channels.

REFERENCES

[1] Hunter, I., Billonet, L., Jarry, B., and Guillon, P., "Microwave Filters—Applications and Technology", *IEEE Trans. Microwave Theory & Tech.*, vol. 50, no. 3, pp. 794-805, March 2002.

[2] Rauscher, C., "Efficient Design Methodology for Microwave Frequency Multiplexers Using Infinite-Array Prototype Circuits", *IEEE Trans. Microwave Theory & Tech.*, vol. 42, no. 7, pp. 1337-1346, July 1994.

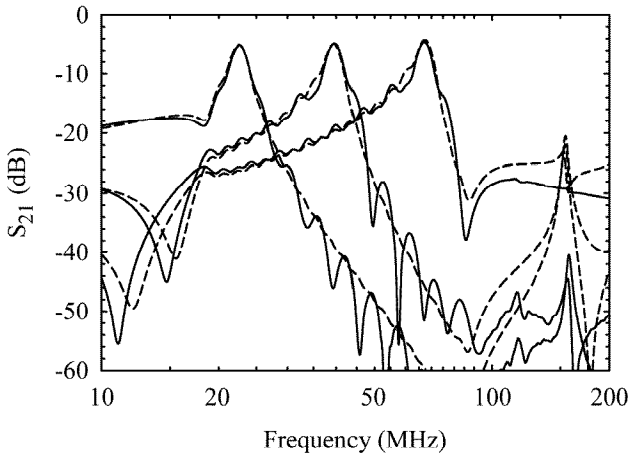

Fig. 9. Measured (solid) and simulated (dashed) S_{n1} of the channelizing filter for channels 3 (left), 10 (center), and 17 (right). Ripples are due to parasitics and resonances of the lumped components.

TABLE II
SAMPLE CHANNEL POWER DISTRIBUTION FOR CHANNEL 10

	Power (%)
Channel 10 Output	33.2 (−4.8 dB)
Sum of Channel 1–9, 11–20 Outputs	32.3
Reflected at Input	3.5
Sum of all Power Contributions	69.0
Power Dissipated	31.0

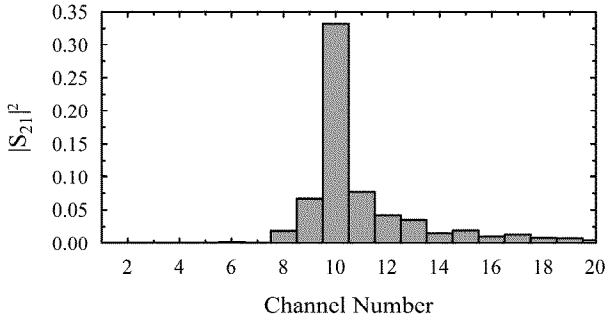

Fig. 10. Power distribution at the center of channel 10 (39.4 MHz) among all 20 channels.

[3] Bekesy, G. V., "Traveling Waves as Frequency Analysers in the Cochlea", *Nature*, 225: pp. 1207-1209, 1970.

[4] Watts, L., "Cochlear Mechanics: Analysis and Analog VLSI", California Institute of Technology, 1993.

[5] Lazzaro, J. and Mead, C., "Circuit Models of Sensory Transduction in the Cochlea", *Analog VLSI Implementation of Neural Networks*, ed. C.a.I. Mead, M, Norwell, MA: Kluwer. 85-101, 1989.

[6] de Boer, E. and van Bienema, E., "Solving cochlear mechanics problems with higher-order differential equations", *Journal of the Acoustical Society of America*, 72 (5), pp. 1427-1434, 1982.

[7] Parthasarathi, A., Grosh, K., and Nuttall, A., "Three-dimensional numerical modeling for global cochlear dynamics", *Journal of the Acoustical Society of America*, 107 (1), pp. 474-485, 2000.